Available online at www.sciencedirect.com
ScienceDirect
Journal of Power Sources 172 (2007) 368–375
JOURNAL OF POWER SOURCES
www.elsevier.com/locate/jpowsour

Characterization of water gas shift reaction in association with carbon dioxide sequestration

Wei-Hsin Chen *, Jian-Guo Jheng

Graduate Institute of Greenergy Technology, National University of Tainan, Tainan 700, Taiwan

Received 31 May 2007; received in revised form 11 July 2007; accepted 11 July 2007
Available online 17 July 2007

Abstract

The characteristics of a water gas shift reaction (WGSR) in association with carbon dioxide sequestration under the effects of a high-temperature catalyst (HTC) and a low-temperature catalyst (LTC) are studied experimentally. With the condition of fixed residence time (0.1 s) for the reactants in the catalyst bed, it is found that the reaction behaviors with the HTC are inherently different from those with the LTC. Specifically, for the WGSR with the HTC, the reaction can be divided into a rapid growth regime, a progressive growth regime and a slow growth regime with increasing reaction temperature or steam/CO ratio. With regard to the WGSR with the LTC, three different regimes are also exhibited; however, they consist of a rapid growth regime, a progressive decay regime and a growth-frozen regime. According to the aforementioned characteristics, proper or better operation conditions using the HTC and the LTC for the application of fuel cells are suggested. When the product gas passes through a $Ca(OH)_2$ solution, the obtained results reveal that CO_2 removal efficiency increases with increasing solution concentration or steam/CO ratio for both the HTC and the LTC used in the WGSR.

Keywords: Water gas shift reaction; Catalyst; Hydrogen; Fuel cell; Carbon dioxide sequestration

1. Introduction

It is well known that hydrogen is a crucial raw material in industry. It has been extensively used for ammonia synthesis, the breaking down of heavier crude oils and the removal of sulfur. In addition to the raw material, hydrogen is also a remarkable fuel for combustion. Its power density, or heating value per unit mass, is much higher than other gases or liquid fuels [1]. For this reason, hydrogen has been employed in liquid rockets and space shuttles as an important propellant for many decades. In the future, seeing that fuel cells are very likely to become an efficient and clean alternative to fuel combustion for primary power generation or distributed generation, it is anticipated that hydrogen will become more and more important as a fuel supply. This implies that the production of hydrogen will be an essential task for the utilization and application of fuel cells and the development of a hydrogen economy [2–4].

As far as hydrogen generation is concerned, the water gas shift reaction (WGSR)

$$CO + H_2O \leftrightarrow CO_2 + H_2 \qquad \Delta H = -41\,\mathrm{kJ\,mol^{-1}} \qquad (1)$$

is a fundamental and important process in nature. This comes from the fact that hydrogen can be produced from water or steam by means of carbon monoxide oxidation into carbon dioxide, as expressed in the preceding equation. During gasification processes, WGSR will simultaneously occur, while partial oxidation reactions of fuels proceed to generate synthesis gas or syngas (i.e. $H_2 + CO$) [5,6]. The concentration of hydrogen in the syngas can be determined by controlling the fuel/steam or the C/H ratio in the feeding stream. After the syngas is produced from the gasification of hydrocarbons, hydrogen concentration can be enriched, through further WGSR procedures. Apart from the gasification, steam reforming is another widely used technique for producing hydrogen [7,8]. This can be practiced from different feedstocks such as methanol, ethanol and methane. Following the reactions of steam reforming, on account of the mixture of CO, CO_2, H_2 and CH_4 contained in the product gas, WGSR can be subsequently carried out to reduce the concen-

* Corresponding author. Tel.: +886 6 2602251; fax: +886 6 2602596.
E-mail address: weihsinchen@gmail.com (W.-H. Chen).

0378-7753/$ – see front matter © 2007 Elsevier B.V. All rights reserved.
doi:10.1016/j.jpowsour.2007.07.022

tration of CO to the level of 0.5% [9] and thereby promote the concentration of H_2. In such a situation it is easier to remove CO using palladium or other membranes to avoid poisoning the platinum-alloy catalysts used in the electrodes of fuel cells [10].

When WGSR is applied for hydrogen generation, the reaction processes can be catalogued into two different ways. One is a reaction in the presence of catalysts and the other is a reaction without the presence of catalysts. The catalytic processes can be further classified into two groups, depending on the reaction temperature or catalyst type. They are the high-temperature shift (HTS) reaction and the low-temperature shift (LTS) reaction. The HTS is usually developed at temperatures ranging from 320 to 450 °C. The LTS is operated at temperatures ranging from 200 to 250 °C [11]. Commercially, iron–chromium-based catalysts are the most widely used catalysts for the HTS reactions [12,13]. Alternatively, copper–zinc-based catalysts have been extensively applied in developing the LTS reactions [14,15]. Aside from the Fe–Cr-based catalysts and the Cu–Zn-based catalysts, gold-based [16] catalysts and platinum group metals [17] can also be used to facilitate the WGSR. However, the prices of gold and platinum are much higher than that of the commercial Fe–Cr or Cu–Zn-based catalysts. Other metals such as zeolite [18] and Sn, Ce, Ru and Rd [19] or B, Cu, Ba, Pb, Hg and Ag [20] imbedded in the catalyst have also been studied to increase the performance of WGSR.

In the absence of catalysts, the WSGR reaction can be triggered when CO is immersed an environment of supercritical water [21–24]. For example, in the kinetics study of Araki et al. [23], they found that the reaction proceeded according to the stoichiometric reaction as $CO + H_2O \rightarrow CO_2 + H_2$, whose rate was first order on the concentration of CO. The rate determining step of the WGSR was the formation process of formic acid, which subsequently dissociated to $CO_2 + H_2$ at a much higher reaction rate. In the experimental study of Sato et al. [24], a non-catalytic WGSR was performed at a CO/H_2O ratio of 0.03 and at temperatures ranging from 653 to 713 K. The first order rate constant of the WGSR was established as well. It was found that the CO conversion rate was relatively low compared to the conventional catalytic processes.

An examination of the aforementioned literature shows that many outstanding studies have been reported. When considering the catalytic process, hydrogen generation from a WGSR is deeply affected by the composition of the catalyst. For this reason, the attentions of the studies were always focused on the preparation of the catalysts and relatively little focus on the performance of the WGSR. In the present study, the characteristics of the WGSR affected by various operational conditions will be explored and described under individual existences of a HTC and a LTC in a reactor. Recognizing the behaviors of the WGSR with the effects of the catalysts, better reaction parameters will be suggested to aid in the production of hydrogen for the application of fuel cells. In addition, by virtue of CO_2 being an important product in a WGSR and the main reason for causing the greenhouse effect, the behaviors of carbon sequestration through CO_2 absorption by $Ca(OH)_2$ solutions will also be investigated.

2. Experimental

Water gas shift reactions (WGSR) were performed by means of a conducted reaction system in this study (schematic of the system is sketched in Fig. 1). As shown in Fig. 1, in the input unit the volumetric flow rate of water was controlled by a rotary pump where a calibration curve of the flow rate was first established. With regard to the feeding gas, the residence time or gas hourly space velocity (GHSV) of the reactants (i.e. H_2O and CO) was fixed in the study. CO and N_2 were blended in a mixer and their flow rates were controlled by use of an electric flow rate controller. The feeding of gas (i.e. $CO + N_2$) and water were

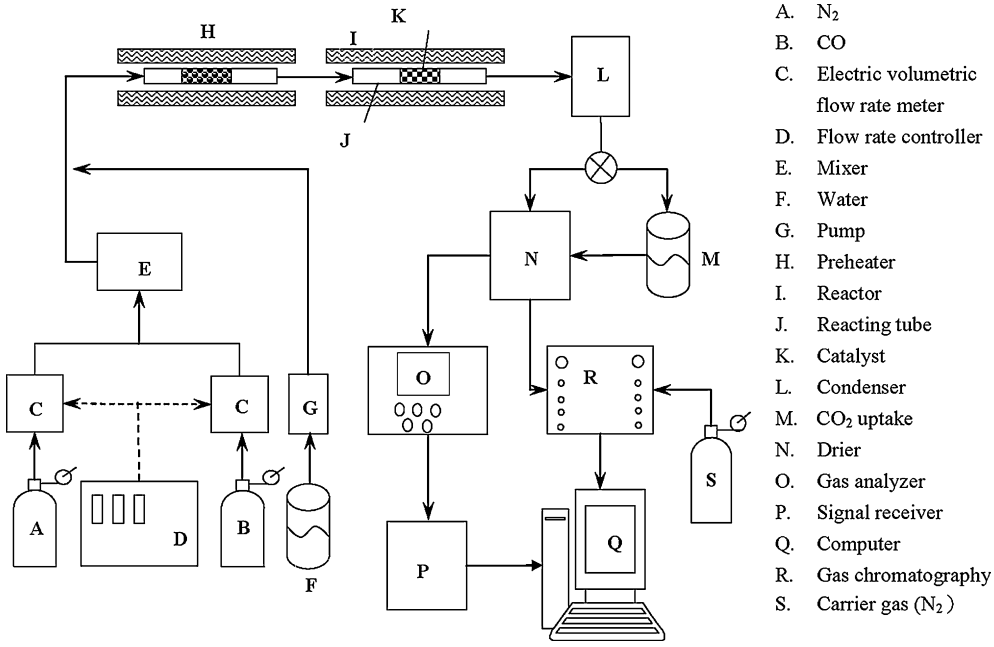

Fig. 1. A schematic of the reaction system.

Table 1
Components of the catalysts and operation conditions for WGSR

Catalyst	Surface area ($m^2\ g^{-1}$)	Component (weight %)	Reaction temperature (°C)	Catalyst bed length (cm)	Residence time (s)	Volumetric flow rate of water ($mL\ min^{-1}$, 25 °C)	Steam/CO ratio
High-temperature catalyst	62.730	Iron oxide: 86–92 Chromium oxide: 6–10 Chromium trioxide: 0.1–2.0 Copper oxide: 1.5–2.1	300–500	8	0.1	0.463	1:1–10:1
Low-temperature catalyst	59.369	Copper Oxide: 40–44 Zinc Oxide: 44–50 Aluminum Oxide: 7.0–13	200–400	8	0.1	0.463	1:1–10:1

simultaneously sent into the preheater in a co-current pattern. Water was heated and transformed into steam which would then be uniformly mixed with the feeding gas. The mixture was then transported into the reactor. Both the preheater and reactor were heated by heating elements. The power of the heating elements was controlled by temperature controllers and power controllers. The tube inside the preheater was filled with glass balls, which were able to absorb heat and uniformly heat the water. Similarly, the tube inside the reactor was packed with catalyst pellets, which could elicit the WGSR. The product gas was then sent to a condenser in which moisture contained in the gas was preliminarily removed. The product gas would then pass through a drier or flow into a $Ca(OH)_2$ solution followed by entering the drier to remove moisture completely. Volumetric concentrations of CO, CO_2 and H_2 were then detected by a gas analyzer (Fuji ZRJF5Y23-AERYR-YKLYYCY-A) and a gas chromatography (GOW-MAC Series 400). The electrical signals from the gas analyzer and gas chromatography were sent into a computer to indicate and record the concentrations of CO, CO_2 and H_2. To ensure the measurement quality, prior to performing experiments, the feeding gas, with a fixed volumetric flow rate, was blown into the reaction system. Then the flow rate of the feeding gas and the concentration of CO were measured at the system exit. This guaranteed that no gas leakage occurred. In addition, the calibrations of the gas analyzer and the gas chromatography were carried out by means of standard gases.

The important parameters affecting WGSR for the study include reaction temperature, catalyst composition, residence time and concentrations of reactants in the catalyst bed. The purpose of the present study is to recognize the characteristics of the HTS and LTS reactions at various reaction temperatures and steam/CO ratios, to provide a useful insight into the production of hydrogen practically. Therefore, two different catalysts, consisting of a high-temperature catalyst (HTC, Sud-Chemie SHT-4) and a low-temperature catalyst (LTC, Sud-Chemie MDC-7), have been adopted to explore the reactions. The components of the two catalysts and their surface areas are shown in Table 1. The scanning electron microscope (SEM, Hitachi

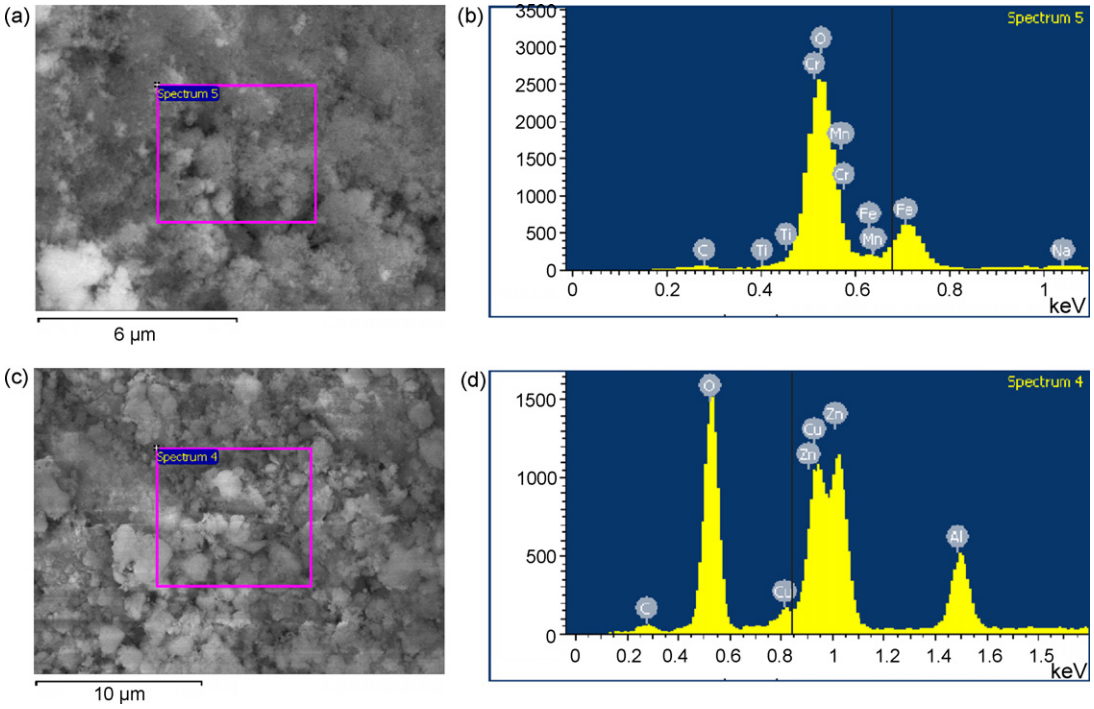

Fig. 2. (a) SEM image and (b) EDS analysis of the high-temperature catalyst as well as (c) SEM image and (d) EDS analysis of the low-temperature catalyst.

S4800) observations and the energy dispersive spectrometer (EDS) analyses of the catalysts are presented in Fig. 2. It is clear from Table 1 and Fig. 2, that the HTC is an iron–chromium-based catalyst, whereas the LTC is a copper–zinc-based catalyst.

3. Results and discussion

In order to provide a basis for comparison, the residence time of the reactants (i.e. $CO + H_2O$) in the catalyst bed will be fixed at 0.1 s (or GHSV = 36,000 h^{-1}). This residence time has been tested and illustrated to show that 0.1 s is long enough for the WGSR to adequately develop. Details of the operational conditions of the experiments are given in Table 1 as well. Based on the required residence time with the catalyst bed porosity of 0.3, the volumetric flow rates of feeding gas (viz., $CO + N_2$) and the volumetric percentages of CO in the feeding gas at various reaction temperatures and steam/CO ratios are provided in Table 2. It can be seen that increasing reaction temperature decreases the volumetric flow rate of the feeding gas, but it increases the volumetric percentage of CO. On the other hand, the volumetric percentage of CO declines as the steam/CO ratio decreases, on account of fixed water volumetric flow rate.

3.1. Product gas concentration

The concentrations of CO, CO_2 and H_2 from WGSR under the effect of the HTC are first presented in Fig. 3, where the reaction temperature varies from 300 to 500 °C and three steam/CO ratios of 1, 4 and 10 are selected. In examining concentration distributions of CO_2 and H_2 shown in Fig. 3a–c, it can be found that their concentrations always rise with increasing reaction temperature, no matter what the steam/CO ratio is. Contrary to the behaviors of CO_2 and H_2, when the steam/CO ratio is 4 or 8, the concentration of CO decays with increasing reaction temperature (Fig. 3b and c). However, when the steam/CO ratio is 1, it is noted that the concentration of CO is characterized by a smiling curve. When the volumetric percentage of CO shown in Table 2 is examined, under the condition of fixed residence time (0.1 s) and steam/CO ratio, it can be seen that the value grows with increasing reaction temperature. Apparently, when the steam/CO ratio is higher such as 4 or 8, the forward reaction of the WGSR is strong enough so that the concentration of CO is reduced as the reaction temperature increases. When the steam/CO ratio is 1 and the reaction temperature is below 400 °C, the aforementioned behavior is still featured. However, once the ratio is higher than 4, the strength of the forward reaction of the WGSR is insufficient to counteract the increase in CO concentration, the smiling curve is exhibited.

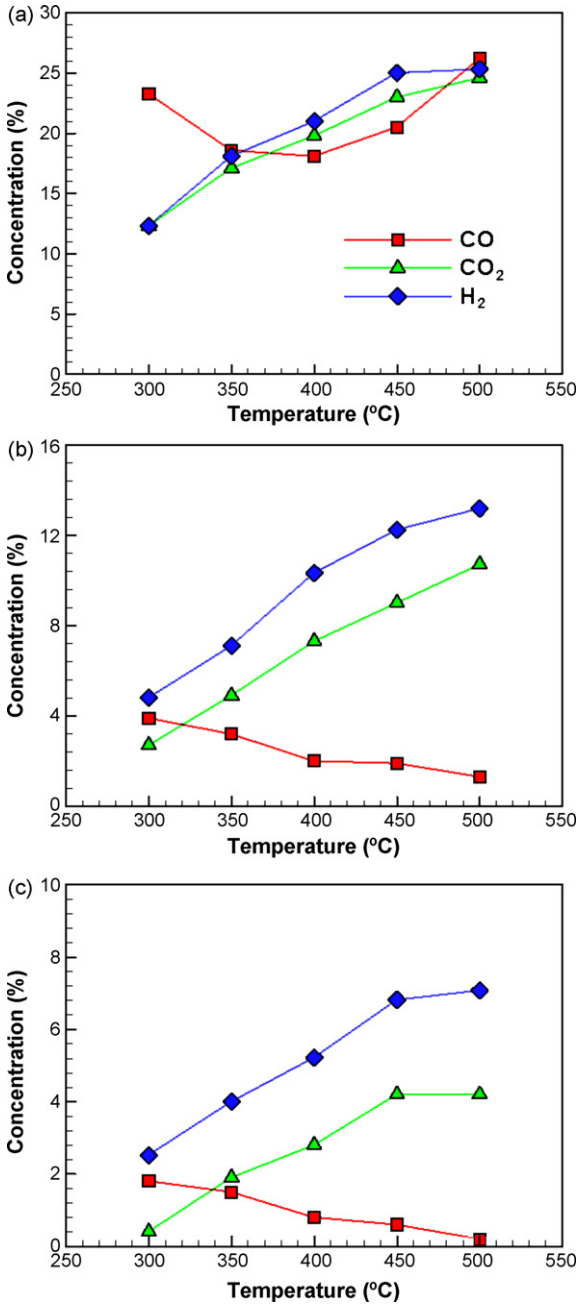

Fig. 3. Volumetric concentration distributions of CO, CO_2 and H_2 under the effect of the HTC at the steam/CO ratios of (a) 1, (b) 4 and (c) 8.

Table 2
Volumetric flow rates of feeding gas and CO volumetric percentages in the feeding gas at various reaction temperatures and steam/CO ratios

Temperature (°C)	Volumetric flow rate of feeding gas (mL min^{-1})	Steam/CO ratio[a]				
		1	4	6	8	10
200	2181	28.86	7.21	4.81	3.61	2.89
250	1912	32.91	8.23	5.48	4.11	3.29
300	1691	37.23	9.31	6.20	4.65	3.72
350	1505	41.83	10.46	6.97	5.23	4.18
400	1346	46.76	11.70	7.79	5.84	4.68
450	1210	52.04	13.01	8.67	6.50	5.20
500	1091	57.71	14.43	9.62	7.21	5.77

[a] CO volumetric percentage in feeding gas (%).

When attention is paid to the behavior of the WGSR with the effect of the LTC, Fig. 4 displays the concentrations of CO, CO_2 and H_2 where the reaction temperature is in the range of 200 and 400 °C and the steam/CO ratios are 1, 4 and 8. As a whole, though the concentrations of CO_2 and H_2 increase with increasing reaction temperature, the concentration of CO is promoted as well, unlike the behavior of CO shown in Fig. 3. This reveals

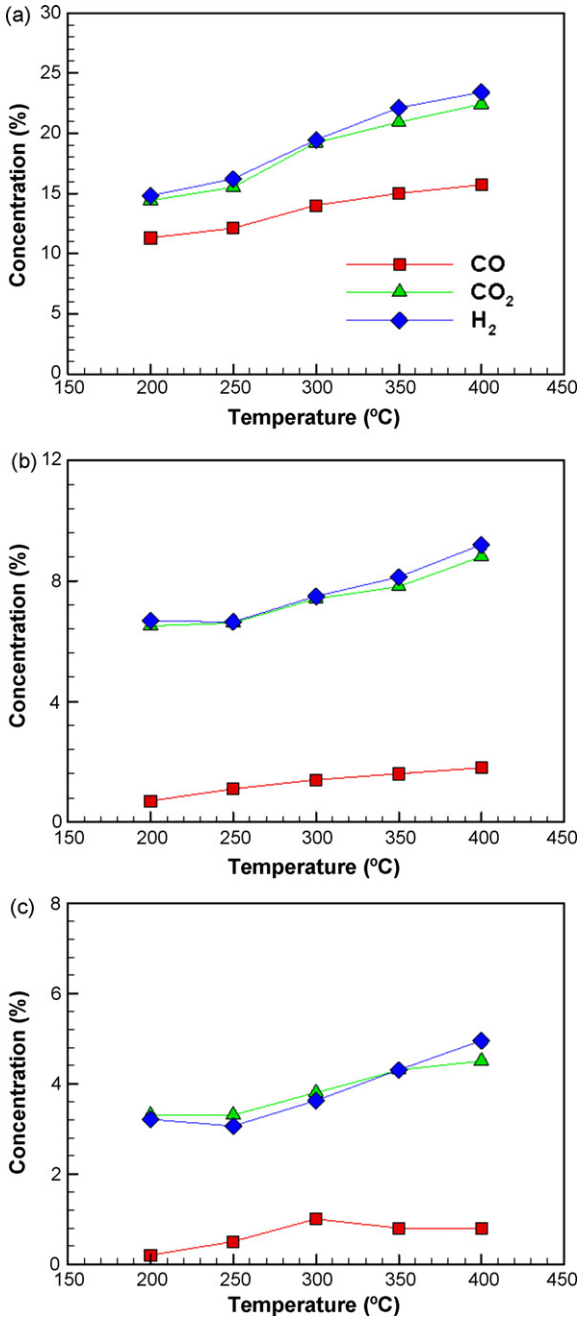

Fig. 4. Volumetric concentration distributions of CO, CO_2 and H_2 under the effect of the LTC at the steam/CO ratios of (a) 1, (b) 4 and (c) 8.

that, with the effect of the LTC, an increase in reaction temperature does not absolutely enhance the performance of the WGSR, resulting from CO conversion being determined by CO and CO_2 concentrations. Hence, the characteristic of the WGSR with the effect of the HTC is dramatically different from that with the effect of the LTC.

3.2. CO conversion

As far as the performance of the WGSR is concerned, the efficiency of hydrogen generation can be represented by CO conversion. The higher the CO conversion, the more hydrogen

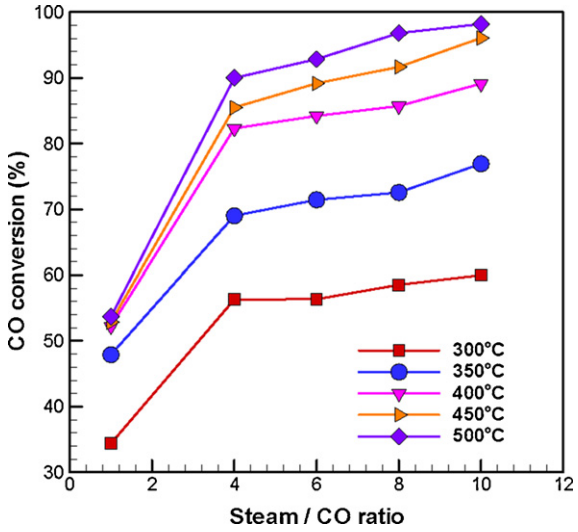

Fig. 5. Distributions of CO conversion with respect to steam/CO ratio at various reaction temperatures for WGSR with the effect of the HTC.

produced. To figure out the reaction performance with varying steam/CO ratios, the values of CO conversion with the effects of the HTC and the LTC are demonstrated in Figs. 5 and 6, respectively. When the reaction temperature is 300 °C where the HTC is used (Fig. 5), an increase in steam/CO ratio is conducive to achieving a higher production of hydrogen. However, the CO conversion ranges from 34% to 60%, implying that the performance of the WGSR is relatively poor. Once the reaction temperature is increased to 350 °C, a significant improvement in CO conversion is the result. Specifically, the CO conversion is between 48% and 77%. Nevertheless, the performance of the WGSR is still relatively low. With increasing the reaction temperature further, up to 400 °C, the CO conversion can be lifted up to 89% which occurs at the steam/CO ratio of 10. However, when the reaction temperature is pushed to 450 or 500 °C, the extent of improvement tends to decay, in spite of further enhancement in CO conversion. This result is not as signifi-

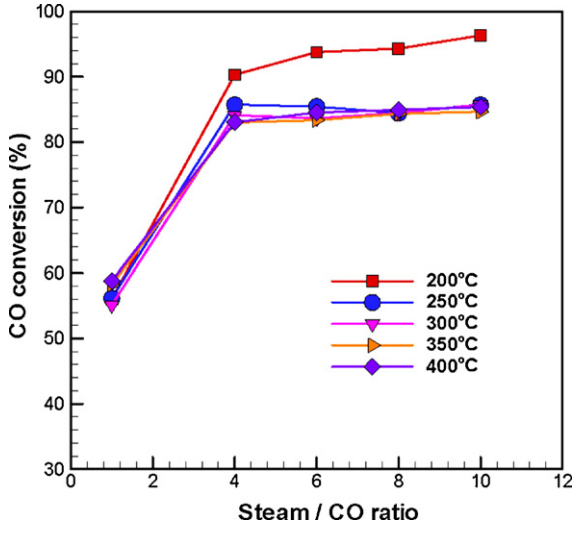

Fig. 6. Distributions of CO conversion with respect to steam/CO ratio at various reaction temperatures for WGSR with the effect of the LTC.

cant as those performed at lower reaction temperatures. As a whole, increasing both reaction temperature and steam/CO ratio increases the performance of the WGSR.

When the performance of the WGSR with the effect of LTC is considered, Fig. 6 displays the distributions of CO conversion at various reaction temperatures where the steam/CO ratio varies from 1 to 10. From the distributions, it is noteworthy that the CO conversion is fairly different from that shown in Fig. 5. For example, the CO conversion at 200 °C is relatively high when compared with the other reaction temperatures, with the exception of steam/CO ratio of 1. It follows that at 200 °C hydrogen production increases with increasing steam/CO ratio. Yet, when the reaction temperature is as high as 250 °C, increasing either reaction temperature or steam/CO ratio does not give an advantage to the CO conversion nor the hydrogen generation, excepting the steam/CO ratio between 1 and 4. It is thus recognized that there is an essential difference in reaction characteristics between using the HTC and the LTC, and an optimal reaction temperature exists when the LTC is employed.

3.3. Characterization of WGSR

To proceed farther into the recognition of WGSR characteristics, a three-dimensional profile of CO conversion versus reaction temperature and steam/CO ratio under the effect of the HTC is provided in Fig. 7a. From the profile shown in Fig. 7, when the steam/CO ratio increases from 1 to 4, the CO conversion greatly increases no matter what the temperature is. When the steam/CO ratio goes beyond 4 and the reaction temperature is between 300 and 400 °C, the growth of CO conversion with increasing temperature is also exhibited, but the growth extent is not as significant as that in the aforementioned regime. On the other hand, when the steam/CO ratio is higher than 4 and the reaction temperature is higher than 400 °C, Fig. 7a depicts that the growth of CO conversion tends to wither. This shows that there are three different regimes in accordance with the growth of CO conversion (or hydrogen generation) that can be identified. In the first regime where the steam/CO is below 4 and the reaction temperature ranges from 300 to 500 °C, the WGSR is located at a rapid growth area, as shown in Fig. 7b. In the second regime where the steam/CO ratio is beyond 4 and the temperature is between 300 and 400 °C, the CO conversion is characterized by a progressive growth. In the third regime where the steam/CO ratio is larger than 4 and the temperature is higher than 400 °C, a slow growth in CO conversion is featured. From the viewpoint of practical WGSR operation, an increase in steam/CO ratio is conducive to CO conversion, as shown in Fig. 5. However, increasing steam also means that more heat is required to transform water into steam, thereby more energy is wasted. Accordingly, Figs. 5 and 7a reflect that the boundary

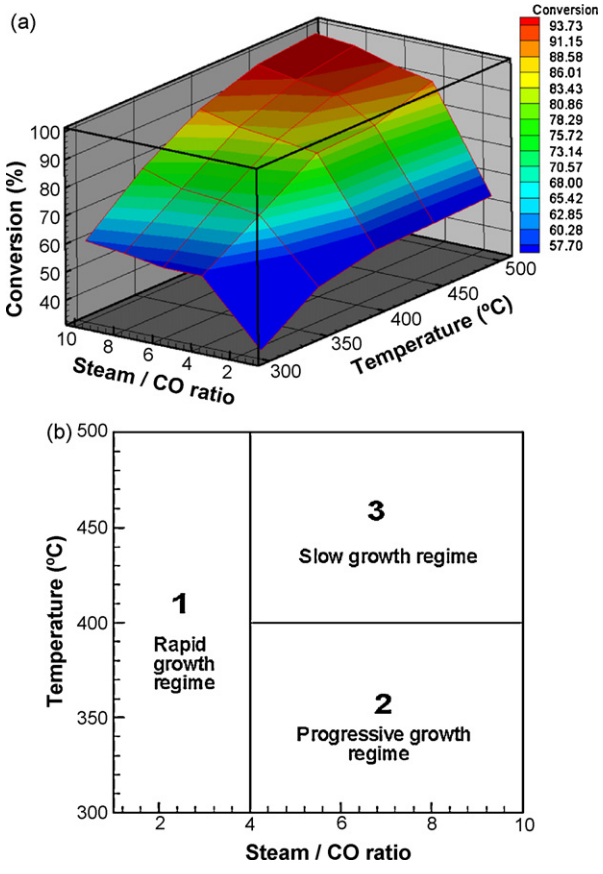

Fig. 7. (a) Three dimensional profile of CO conversion and (b) regime locations of WGSR characteristic under the effect of the HTC.

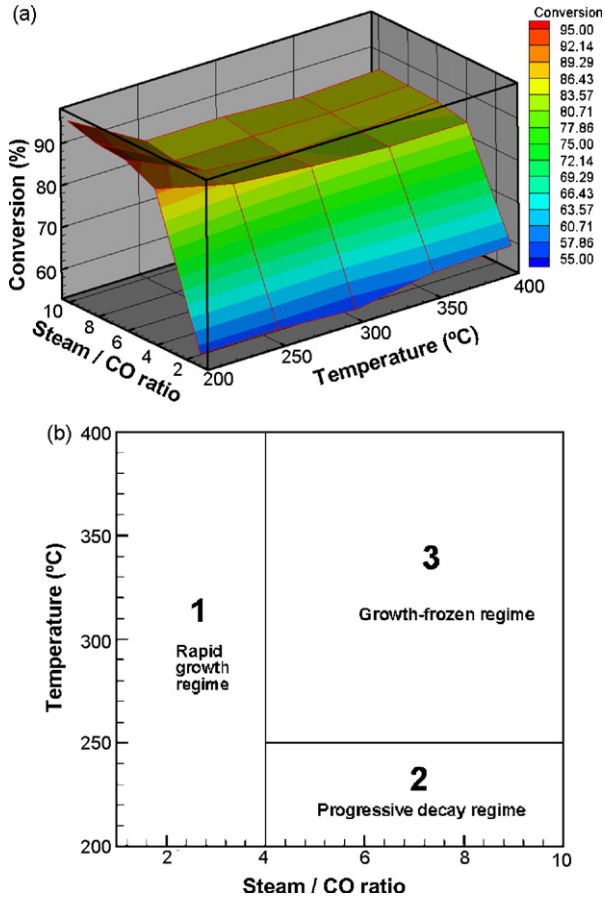

Fig. 8. (a) Three dimensional profile of CO conversion and (b) regime locations of WGSR characteristic under the effect of the LTC.

between the first regime and the third regime will be the better operation condition.

Fig. 8a sketches a three-dimensional profile of the CO conversion from WGSR with the effect of the LTC. When the steam/CO ratio is increased from 1 to 4 (the first regime), the CO conversion is characterized by a rapid growth, whatever the reaction temperature is encountered. This result resembles that shown in Fig. 7a. When the steam/CO ratio is beyond 4 and the reaction temperature is increased from 200 to 250 °C (the second regime), the CO conversion declines progressively with increasing reaction temperature. This implies that the increase of reaction temperature inhibits the WGSR. For the cases of steam/CO ratio beyond 4 and reaction temperature beyond 250 °C (the third regime), the distribution of the CO conversion behaves as a plain with increasing reaction temperature or steam/CO ratio. In other words, hydrogen generation is almost independent of the ratio and the temperature in this regime. From the above observations, the entire reaction characteristics can also be grouped into three regimes. In the first regime (steam/CO ≤ 4 and temperature = 200–400 °C), the WGSR belongs to a rapid growth mode. In the second regime (steam/CO > 4 and temperature = 200–250 °C), the reaction is governed by a progressive decay mode. In the third regime (steam/CO > 4 and temperature = 250–400 °C), the reaction intrinsically pertains to a growth-frozen mode, as shown in Fig. 8b. From the distributions shown in Figs. 6 and 8b, a better or optimal operational condition at the reaction temperature of 200 °C and the steam/CO ratio of 4 is suggested.

From the above results, it has been known that increasing steam/CO ratio can promote the CO conversion percentage, but the overall thermal efficiency of the reaction system may decline, as described before. As a matter of fact, the overall thermal efficiency will be affected by some important parameters such as reaction temperature, steam/CO ratio and residence time of the reactants in a catalyst bed. Therefore, the analysis of the overall thermal efficiency is worthy of study in the future.

3.4. Carbon dioxide sequestration

In a WGSR, carbon dioxide is another important product. If CO_2 is removed from the product gas, the concentration of hydrogen will be enlarged so as to increase the utilization of hydrogen in fuel cells. For this reason, following the WGSR, the product gas is injected into a $Ca(OH)_2$ solution to account for the behavior of CO_2 sequestration. The distributions of CO_2 removal percentage from the product gas of the HTS reactions at various molar concentrations of the solution (1–5 M) are displayed in Fig. 9. The solution temperature is at room temperature. The curves shown in Fig. 9a depict that the CO_2 removal percentage increases with increasing the steam/CO ratio for all the solution concentrations. This result is a consequence of two factors; they include less CO_2 contained in the prod-

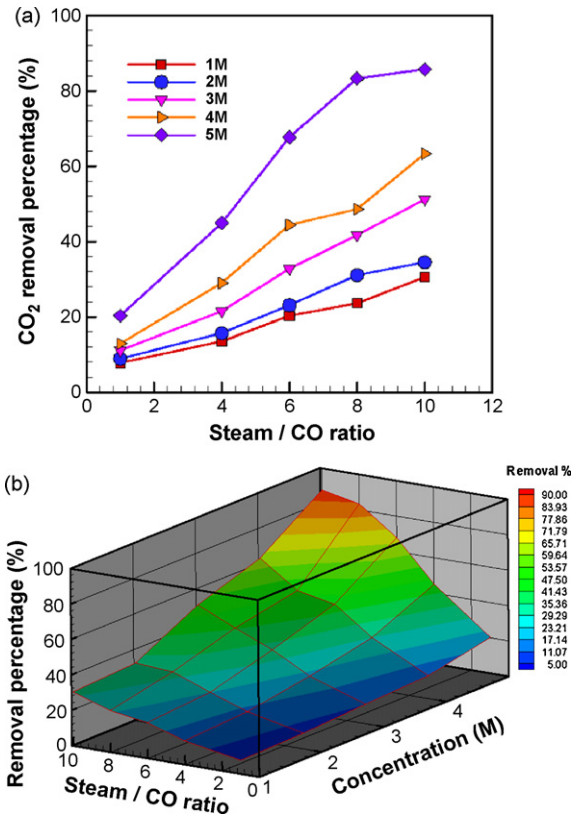

Fig. 9. (a) Two-dimensional and (b) three-dimensional distributions of CO_2 removal percentage at various steam/CO ratios and solution concentrations for WGSR with the effect of the HTC.

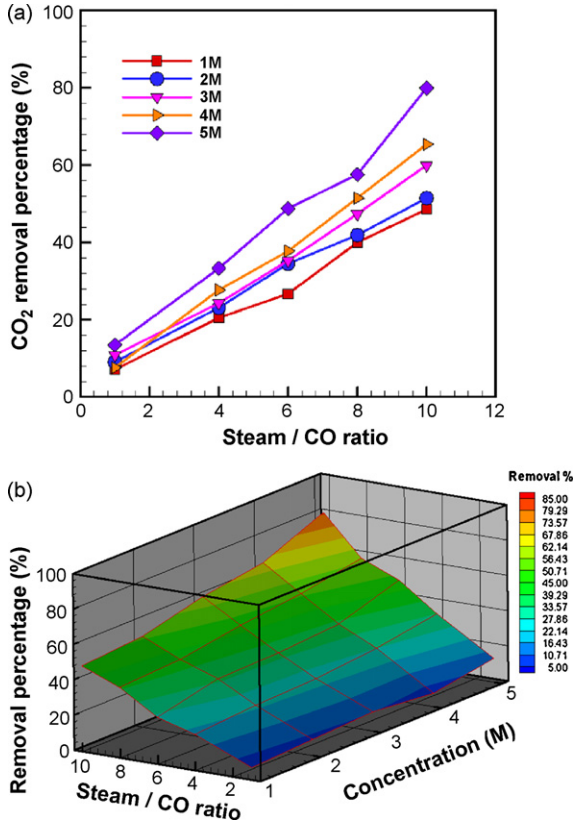

Fig. 10. (a) Two-dimensional and (b) three-dimensional distributions of CO_2 removal percentage at various steam/CO ratios and solution concentrations for WGSR with the effect of the LTC.

uct gas and a relatively higher CO conversion as the steam/CO ratio increases. Although a higher steam/CO ratio will enhance the CO conversion, the formed CO_2 concentration in the product gas is still lower than that from lower steam/CO ratios (see Table 2). Fig. 9a also shows that an increase in the concentration of a $Ca(OH)_2$ solution will enhance the CO_2 removal. When examining the three-dimensional profile of the CO_2 removal percentage shown in Fig. 9b, the best removal efficiency occurs at the steam/CO ratio of 10 and the concentration of 5 M, where the removal efficiency is 86%. Upon inspection of CO_2 removal from the LTS reactions, basically, as shown in Fig. 10a and b, the behaviors are similar to that from the HTS reactions. When the steam/CO ratio is between 4 and 10, the enhancement of CO_2 removal with increasing steam/CO ratio mainly results from lower CO_2 concentration contained in the product gas because the CO conversion is located in the growth-frozen regime (Fig. 6).

4. Conclusions

By establishing a WGSR system in cooperation with using the HTC and LTC, the characteristics of CO conversion and hydrogen generation from water gas shift reactions have been investigated and outlined. When the HTC was employed, the CO conversion was featured by three different regimes with increasing reaction temperature or steam/CO ratio. They were the rapid growth regime, progressive growth regime and slow growth regime. Unlike the proceeding characteristics, the behavior of the WGSR with the effect of the LTC was characterized by the rapid growth regime, progressive decay regime and growth-frozen regime. Better operational conditions for the HTC to be used in the WGSR are suggested at the steam/CO ratio of 4 and temperature between 400 and 500 °C, whereas the steam/CO ratio of 4 and temperature of 200 °C is suggested for the optimal operation of the LTC. Despite substantially different behaviors exhibited using the HTC and LTC, the basic characteristics of CO_2 removed by $Ca(OH)_2$ solution are similar, regardless of the catalysts used. In addition to the aforementioned operations, if the WGSR is performed in a membrane reactor, the reaction product can be removed directly from the reaction system. As a result, the removal of the product can further promote the WGSR toward the product side in accordance with the thermodynamic equilibrium. Then, one is able to increase the CO conversion percentage as well.

Acknowledgements

The authors wish to express their gratitude to the National Science Council and the Bureau of Energy, Ministry of Economic Affairs, Taiwan, ROC, for supporting this research.

References

[1] C.K. Law, Combustion Physics, Cambridge, New York, USA, 2006.
[2] U.S. Department of Energy (DOE), A National Vision of America's Transition to a Hydrogen Economy—To 2030 and Beyond, February 2002.
[3] L. Barreto, A. Makihira, K. Riahi, Int. J. Hydrogen Energy 28 (2003) 267–284.
[4] J.W. Phair, S.P.S. Badwal, Ionics 12 (2006) 103–115.
[5] W.H. Chen, J.C. Chen, C.D. Tsai, T.L. Jiang, Int. J. Energy Res. 31 (2007) 895–911.
[6] C. Higman, M. Van der Burgt, Gasification, Elsevier, New York, USA, 2003.
[7] Z.W. Liu, K.W. Jun, H.S. Roh, S.E. Park, J. Power Sources 111 (2002) 283–287.
[8] A.Y. Tonkovich, S. Perry, Y. Wang, D. Qiu, T. LaPlantea, W.A. Rogers, Chem. Eng. Sci. 59 (2004) 4819–4824.
[9] W. Ruettinger, O. Ilinich, R.J. Farrauto, J. Power Sources 118 (2003) 61–65.
[10] Y.M. Lin, M.H. Rei, Catal. Today 67 (2001) 77–84.
[11] F. Bustamante, The High-Temperature, High-Pressure Homogeneous Water–Gas Shift Reaction in a Membrane Reactor. University of Pittsburgh, Ph.D. Thesis, 2004.
[12] J.L.R. Costa, G.S. Marchetti, M.C. Rangel, Catal. Today 77 (2002) 205–213.
[13] R.E. Johnsen, A.M. Molenbroek, K. Stahl, J. Appl. Crystallogr. 39 (2006) 519–526.
[14] K.M. Vanden Bussche, G.F. Froment, J. Catal. 161 (1996) 1–10.
[15] Y. Choi, H.G. Stenger, J. Power Sources 124 (2003) 432–439.
[16] D. Cameron, R. Holliday, D. Thompson, J. Power Sources 118 (2003) 298–303.
[17] D. Tibiletti, F.C. Meunier, A. Goguet, D. Reid, R. Burch, M. Boaro, M. Vicario, A. Trovarelli, J. Catal. 244 (2006) 183–191.
[18] T.R.O. Souza, S.M.O. Brito, H.M.C. Andrade, Appl. Catal. B 178 (1999) 7–15.
[19] A. Basinska, R. Klimkiewicz, H. Teterycz, React. Kinet. Catal. Lett. 82 (2004) 271–277.
[20] C. Rhodes, B.P. Williams, F. King, G.J. Hutchings, Catal. Commun. 3 (2002) 381–384.
[21] R.K. Helling, J.W. Tester, Energy Fuel. 1 (1987) 417–423.
[22] R.H. Holgate, P.A. Webley, J.W. Tester, R.K. Helling, Energy Fuel. 6 (1992) 586–597.
[23] K. Araki, H. Fujiwara, K. Sugimoto, Y. Oshima, S. Koda, J. Chem. Eng. Jpn. 37 (2004) 443–448.
[24] T. Sato, S. Kurosawa, R.L. Smith, T. Adschiri, K. Arai, J. Supercrit. Fluids 29 (2004) 113–119.